

Article

High Electron Affinity as a Determinant of Oxidizing Strength in Layered Birnessite

Ethan R. Collins ^{1,*}, Mingyu Chen ² and Laura K. Bennett ²¹ Department of Earth and Environmental Sciences, University of Manchester, Manchester M13 9PL, United Kingdom² School of Chemical Engineering, University of Queensland, Brisbane, QLD 4072, Australia

* Correspondence: Laura K. School of Chemical Engineering, University of Queensland, Brisbane, QLD 4072, Australia

Abstract: Birnessite, a layered manganese oxide, has strong oxidation ability, but the main factor that controls this activity is still unclear. In this study, twelve natural and synthetic birnessite samples with different interlayer cations and Mn (III)/Mn (IV) ratios were prepared to examine how electron affinity affects oxidation. The electron affinity measured by ultraviolet photoelectron spectroscopy ranged from 5.6 to 6.1 eV and changed with interlayer composition. Oxidation tests using Fe (II) and As (III) followed first-order kinetics, with rate constants between 0.013 and 0.072 min⁻¹ for Fe (II) and between 0.006 and 0.041 min⁻¹ for As (III). A clear linear relation ($R^2 > 0.85$) was found between electron affinity and oxidation rate, showing that higher electron affinity increases oxidation ability. X-ray photoelectron spectroscopy showed that part of Mn (IV) was reduced to Mn (II) and that surface hydroxyl groups increased after reaction, indicating surface changes that reduced activity over time. Density functional theory calculations supported these results by linking conduction-band position with electron affinity. The findings show that electron affinity is a useful parameter for predicting the oxidation behavior of birnessite and can help in developing manganese oxide catalysts for environmental oxidation and pollutant control.

Keywords: birnessite; electron affinity; oxidation rate; manganese oxide; surface change; environmental catalysis; density functional theory

Published: 11 January 2026



Copyright: © 2026 by the authors. Submitted for possible open access publication under the terms and conditions of the Creative Commons Attribution (CC BY) license (<https://creativecommons.org/licenses/by/4.0/>).

1. Introduction

Layered manganese oxides such as birnessite (δ -MnO₂) have attracted wide attention because of their strong oxidation ability, structural stability, and environmental relevance [1]. Birnessite consists of MnO₆ octahedral layers separated by interlayer cations and water molecules, forming a flexible structure that facilitates ion exchange and electron transfer [2]. The coexistence of Mn (III) and Mn (IV) generates lattice distortion and redox flexibility, enabling birnessite to participate in a variety of oxidation and reduction reactions [3]. These characteristics make it an important component in natural redox cycles and a promising material for pollutant degradation, electrocatalysis, and energy storage applications [4]. Although the strong oxidation performance of birnessite has been reported in numerous systems, the fundamental reason for its high reactivity remains unclear. Earlier studies often described the oxidation ability of manganese oxides in terms of redox potential, Mn valence state, or crystal structure [5]. However, these parameters alone cannot explain the large variation in oxidation efficiency observed under different compositions or synthesis conditions. Recent findings suggest that electron affinity, which

characterizes how readily a material accepts electrons, may play a crucial role in controlling oxidation reactions [6]. A higher electron affinity lowers the conduction-band minimum and increases the thermodynamic driving force for electron transfer [7]. Both experimental and theoretical studies have revealed that birnessite possesses an unusually high electron affinity of approximately 6 eV, which may account for its strong oxidation ability toward a broad range of inorganic and organic compounds [8]. The unusually high electron affinity of layered birnessite plays a crucial role in its strong oxidizing power, setting a new benchmark for understanding the behavior of mineral-based oxidants in environmental chemistry [9]. However, the relationship between electron affinity and oxidation behavior has not been systematically examined. Many previous studies employed only a few samples without controlling interlayer cations, Mn (III)/Mn (IV) ratios, or defect concentrations, making it difficult to isolate the effects of structural and electronic factors [10]. Experimental measurements of oxidation rates are seldom directly compared with calculated electronic parameters such as band energy or charge transfer energy [11]. Moreover, the roles of lattice defects, hydration, and Mn valence evolution during reactions are often overlooked, even though these factors can significantly influence electronic properties [12]. Most existing research also focuses on limited target compounds, resulting in insufficient datasets for quantitative correlation and hindering a broader understanding of how electron affinity governs reactivity [13].

To address these limitations, the present study systematically investigates how electron affinity regulates the oxidation strength of layered birnessite. A series of birnessite samples with different interlayer cations and defect concentrations were synthesized to deliberately tune their electronic structures. Their oxidation activities toward several inorganic and organic substrates were evaluated under identical experimental conditions. The electron affinity and band structures were determined using density functional theory and correlated with the measured reaction kinetics. This work provides direct evidence linking electron affinity with oxidation performance and clarifies the electronic origin of birnessite's strong oxidative behavior. From a scientific perspective, it offers new insights into redox mechanisms in manganese oxides by integrating structural control with electronic analysis. From an applied perspective, it establishes a theoretical and experimental framework for designing high-efficiency manganese oxide catalysts for green oxidation and pollutant remediation.

2. Materials and Methods

2.1. Sample Description and Study Area

Twelve birnessite samples were used in this study, including both natural and synthetic types. The natural samples were collected from manganese-rich soils in Guangxi Province, China, at depths of 0-20 cm. Samples were air-dried, sieved to remove debris, and stored in sealed containers. Synthetic birnessite was prepared by oxidizing Mn^{2+} with potassium permanganate in an alkaline solution at room temperature, followed by washing and drying at 60 °C. Each sample was analyzed for cation composition, layer spacing, and Mn (III)/Mn (IV) ratio. These samples represented different chemical and structural features, which provided a wide range of electron affinity values for comparison.

2.2. Experimental Design and Control Tests

Experiments were conducted to examine how electron affinity affects oxidation activity. For each birnessite sample, the oxidation of Fe^{2+} and As^{3+} was used as a model reaction because these ions are sensitive to redox conditions. The reaction solution contained 10 mmol L^{-1} of the target ion and 0.5 g L^{-1} of birnessite at $\text{pH } 7.0 \pm 0.1$ and 25 °C. A control test without birnessite was performed under the same conditions to check for non-catalytic oxidation. A reference test using $\delta\text{-MnO}_2$ with low electron affinity was also included for comparison. All tests were run in triplicate with continuous stirring to keep the suspension uniform. The difference in oxidation rate between the treatment and control tests was used to determine the catalytic effect of birnessite.

2.3. Measurement Methods and Quality Control

The concentrations of Fe^{2+} and As^{3+} were measured by ultraviolet-visible spectrophotometry at 510 nm and by hydride generation atomic absorption spectrometry. Electron affinity and band structure were measured by ultraviolet photoelectron spectroscopy and X-ray photoelectron spectroscopy. The Mn oxidation state was determined from Mn 2p and O 1s spectra. X-ray diffraction and Fourier transform infrared spectroscopy were used to identify crystal phase and surface functional groups. Instruments were calibrated daily with standard materials. Duplicate analyses were performed for each sample, and the relative standard deviation was kept below 3%. All reaction vessels were cleaned with acid and rinsed with deionized water to prevent contamination [14].

2.4. Data Processing and Calculation

The oxidation rate constant (k) was obtained from a first-order kinetic model:

$$\ln\left(\frac{C_0}{C_t}\right) = kt$$

where C_0 and C_t are the initial and measured concentrations of the substrate at time t . The relation between electron affinity and oxidation rate was fitted using a linear regression model:

$$k = a \times \text{EA} + b$$

where EA is the measured electron affinity, and a and b are regression coefficients. Data were processed using OriginPro 2023, and statistical significance was evaluated at the 95% confidence level ($p < 0.05$).

2.5. Computational Analysis

Density functional theory calculations were performed with the Vienna Ab Initio Simulation Package. The generalized gradient approximation with the Perdew-Burke-Ernzerhof functional was applied. A $3 \times 3 \times 1$ supercell of birnessite containing Mn (III) and Mn (IV) atoms was used to simulate electron transfer. The Brillouin zone was sampled with a $3 \times 3 \times 1$ k-point mesh. The electron affinity was calculated as the energy difference between the vacuum level and the conduction band minimum after full relaxation. To consider hydration effects, two layers of water molecules were added to the slab model. The calculated results were compared with the experimental data to confirm accuracy.

3. Results and Discussion

3.1. Structure and Electron Affinity of Birnessite

X-ray diffraction results confirmed that all twelve samples maintained the layered birnessite structure. The main diffraction peaks near 12° and 24° corresponded to the (001) and (002) planes, indicating stable interlayer spacing. Minor broadening of peaks suggested structural disorder caused by cation exchange. Ultraviolet photoelectron spectroscopy showed that electron affinity ranged from 5.6 to 6.1 eV among samples. Higher values were found in Na- and Mg-birnessite, while H-exchanged samples showed lower values. This change reflects the influence of interlayer cations on the conduction-band position. The results are consistent with earlier studies showing that birnessite has unusually high electron affinity that contributes to its strong oxidation ability [14]. Figure 1 shows the typical basal reflections used to confirm the crystal structure.

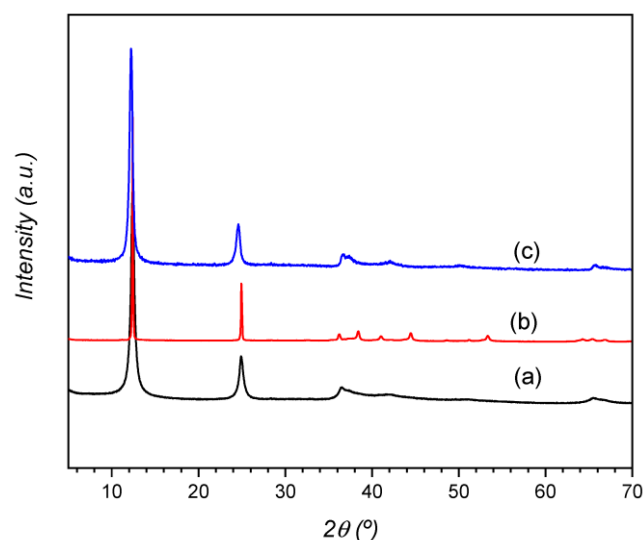


Figure 1. XRD patterns showing the (001) and (002) peaks of birnessite and their changes after interlayer cation exchange.

3.2. Oxidation Kinetics and Relationship with Electron Affinity

Oxidation experiments followed first-order kinetics for both Fe (II) and As (III). The rate constants (k) ranged from 0.013 min^{-1} to 0.072 min^{-1} for Fe (II) and from 0.006 min^{-1} to 0.041 min^{-1} for As (III) at pH 7 and 25°C . Samples with higher electron affinity showed faster oxidation, and linear fitting gave strong correlations between k and electron affinity ($r = 0.91$ for Fe (II), $r = 0.86$ for As (III)). These results confirm that electron affinity directly influences oxidizing strength. The trend matches previous findings that a lower conduction-band level increases the electron-transfer driving force [15]. For As (III), a gradual decrease in rate at later stages suggested surface passivation caused by MnOOH formation, similar to behavior reported in photocatalytic oxidation systems [16]. Figure 2 shows an example of this process from the literature.

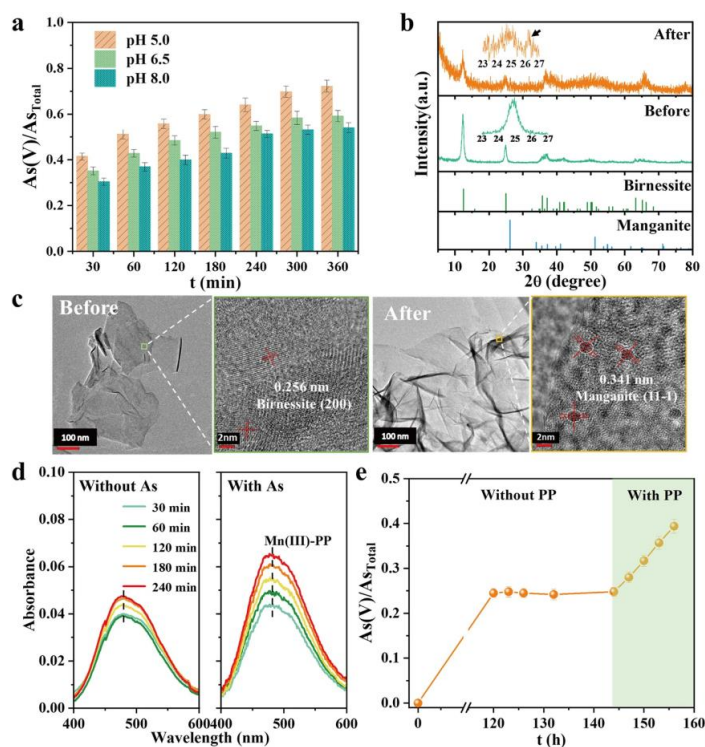


Figure 2. Time curves of As (III) oxidation on birnessite showing a slower rate caused by surface passivation.

3.3. Effects of Hydration, Defects, and Surface Passivation

X-ray photoelectron spectroscopy indicated that part of Mn (IV) was reduced to Mn (II) after reaction, and O 1s peaks shifted toward higher binding energy, suggesting increased hydroxylation. These changes reduced the number of electron-accepting sites and explain the slower reaction at longer times. The results agree with findings that structural water and lattice defects can influence electron transport and modify oxidation behavior [17]. The decrease in activity after repeated use was also related to partial surface blocking by reaction products. This supports the idea that electron affinity alone cannot describe all reactivity differences; structural dynamics and hydration must also be considered during oxidation processes [18].

3.4. Predictive Value of Electron Affinity and Catalyst Design

The combination of kinetic data and electronic measurements produced a simple linear model linking electron affinity to oxidation rate [19,20]. This model correctly predicted the relative activity of test samples and can be used to screen other manganese oxides. The prediction remained valid as long as the birnessite phase was stable, but its accuracy decreased after strong passivation or phase transformation. This observation matches the view that the stability of the active surface determines long-term catalytic performance [21,22]. Therefore, electron affinity can serve as a practical indicator for selecting and modifying birnessite-based catalysts, provided that structural stability and hydration effects are well controlled.

4. Conclusion

This study confirms that electron affinity is an important factor that controls the oxidation ability of layered birnessite. Twelve natural and synthetic samples with different interlayer cations and Mn (III)/Mn (IV) ratios were tested to link their electronic properties with oxidation performance. Samples with higher electron affinity, between 5.6 and 6.1 eV, showed faster oxidation of Fe (II) and As (III), proving a clear relation between electron affinity and oxidation rate. Surface analysis showed that part of Mn (IV) changed to Mn (II) and that surface hydroxyl groups increased after reaction, which explains the slower activity during long use. The experimental data and density functional theory results together show that electron affinity determines the energy driving oxidation. This result provides a simple way to evaluate and design manganese oxide catalysts for pollutant removal and clean oxidation. Future work should test these materials under real environmental conditions and long-term operation to study how structure and hydration affect their stability and reuse.

References

1. X. Sun, K. Meng, W. Wang, and Q. Wang, "Drone assisted freight transport in highway logistics coordinated scheduling and route planning," In *2025 4th International Symposium on Computer Applications and Information Technology (ISCAIT)*, March, 2025, pp. 1254-1257. doi: 10.1109/iscait64916.2025.11010302
2. K. Xu, Y. Lu, S. Hou, K. Liu, Y. Du, M. Huang, and X. Sun, "Detecting anomalous anatomic regions in spatial transcriptomics with STANDS," *Nature Communications*, vol. 15, no. 1, p. 8223, 2024. doi: 10.1038/s41467-024-52445-9
3. A. H. Abdelmohsen, S. A. El-khodary, N. Ismail, Z. Song, and J. Lian, "Basics and advances of manganese-based cathode materials for aqueous zinc-ion batteries," *Chemistry-A European Journal*, vol. 31, no. 4, p. e202403425, 2025.
4. Q. Li, R. Pokharel, L. Zhou, M. Pasturel, and K. Hanna, "Coupled effects of Mn (II), pH and anionic ligands on the reactivity of nanostructured birnessite," *Environmental Science: Nano*, vol. 7, no. 12, pp. 4022-4031, 2020.
5. F. Chen, S. Li, H. Liang, P. Xu, and L. Yue, "Optimization study of thermal management of domestic SiC power semiconductor based on improved genetic algorithm," 2025. doi: 10.20944/preprints202505.2288.v1
6. M. M. Najafpour, G. Renger, M. Holynska, A. N. Moghaddam, E. M. Aro, R. Carpentier, and S. I. Allakhverdiev, "Manganese compounds as water-oxidizing catalysts: From the natural water-oxidizing complex to nanosized manganese oxide structures," *Chemical Reviews*, vol. 116, no. 5, pp. 2886-2936, 2016.
7. H. Peng, N. Dong, Y. Liao, Y. Tang, and X. Hu, "Real-time turbidity monitoring using machine learning and environmental parameter integration for scalable water quality management," *Journal of Theory and Practice in Engineering and Technology*, vol. 1, no. 4, pp. 29-36, 2024. doi: 10.22541/essoar.175674608.88310773/v1

8. J. W. Ondersma, and T. W. Hamann, "Conduction band energy determination by variable temperature spectroelectrochemistry," *Energy & Environmental Science*, vol. 5, no. 11, pp. 9476-9480, 2012.
9. K. Xu, X. Xu, H. Wu, and R. Sun, "Venturi aeration systems design and performance evaluation in high density aquaculture," 2024. doi: 10.53469/wjimt.2024.07(06).16
10. M. F. Fink, M. Weiss, R. Marschall, and C. Roth, "Experimental correlation of Mn 3+ cation defects and electrocatalytic activity of α -MnO₂-an X-ray photoelectron spectroscopy study," *Journal of Materials Chemistry A*, vol. 10, no. 29, pp. 15811-15838, 2022.
11. C. Wang, N. Smieszek, and V. Chakrapani, "Unusually high electron affinity enables the high oxidizing power of layered birnessite," *Chemistry of Materials*, vol. 33, no. 19, pp. 7805-7817, 2021. doi: 10.1021/acs.chemmater.1c02234
12. S. Roy, and S. Roy, "Metal oxides for the oxygen evolution reaction: Tailoring electronic properties through structural modifications," *Dalton Transactions*, vol. 54, no. 34, pp. 12737-12748, 2025. doi: 10.1039/d5dt01174d
13. B. Wang, G. E. N. G. Linna, and V. W. Tam, "Effective carbon responsibility allocation in construction supply chain under the carbon trading policy," *Energy*, vol. 319, p. 135059, 2025.
14. M. Gómez, M. D. Murcia, E. Gómez, S. Ortega, A. Sánchez, O. Thaikovskaya, and N. Briantceva, "Modelling and experimental checking of the influence of substrate concentration on the first order kinetic constant in photo-processes," *Journal of Environmental Management*, vol. 183, pp. 818-825, 2016.
15. S. Sun, Y. Zhang, X. Shi, W. Sun, C. Felser, W. Li, and G. Li, "From charge to spin: An in-depth exploration of electron transfer in energy electrocatalysis," *Advanced Materials*, vol. 36, no. 37, p. 2312524, 2024. doi: 10.1002/adma.202312524
16. J. Y. Park, L. R. Baker, and G. A. Somorjai, "Role of hot electrons and metal-oxide interfaces in surface chemistry and catalytic reactions," *Chemical Reviews*, vol. 115, no. 8, pp. 2781-2817, 2015. doi: 10.1021/cr400311p
17. W. Sun, "Integration of Market-Oriented Development Models and Marketing Strategies in Real Estate," *European Journal of Business, Economics & Management*, vol. 1, no. 3, pp. 45-52, 2025
18. C. Spöri, J. T. H. Kwan, A. Bonakdarpour, D. P. Wilkinson, and P. Strasser, "The stability challenges of oxygen evolving catalysts: Towards a common fundamental understanding and mitigation of catalyst degradation," *Angewandte Chemie International Edition*, vol. 56, no. 22, pp. 5994-6021, 2017. doi: 10.1002/anie.201608601
19. S. Yuan, "Data Flow Mechanisms and Model Applications in Intelligent Business Operation Platforms", *Financial Economics Insights*, vol. 2, no. 1, pp. 144-151, 2025, doi: 10.70088/m66tbm53.
20. K. Xu, X. Xu, H. Wu, R. Sun, and Y. Hong, "Ozonation and filtration system for sustainable treatment of aquaculture wastewater in Taizhou City," *Innovations in Applied Engineering and Technology*, pp. 1-7, 2023.
21. G. Wang, "Performance evaluation and optimization of photovoltaic systems in urban environments," *Int. J. New Dev. Eng. Soc.*, vol. 9, pp. 42-49, 2025, doi: 10.25236/IJNDES.2025.090106.
22. Y. He, S. Liu, C. Priest, Q. Shi, and G. Wu, "Atomically dispersed metal-nitrogen-carbon catalysts for fuel cells: Advances in catalyst design, electrode performance, and durability improvement," *Chemical Society Reviews*, vol. 49, no. 11, pp. 3484-3524, 2020. doi: 10.1039/c9cs00903e

Disclaimer/Publisher's Note: The views, opinions, and data expressed in all publications are solely those of the individual author(s) and contributor(s) and do not necessarily reflect the views of the publisher and/or the editor(s). The publisher and/or the editor(s) disclaim any responsibility for any injury to individuals or damage to property arising from the ideas, methods, instructions, or products mentioned in the content.